JFM RAPIDS
journals.cambridge.org/rapids

Retraction of large liquid strips

Cunjing Lv[1], Christophe Clanet[1,2] and David Quéré[1,2],†

[1]PMMH, CNRS UMR 7636, ESPCI, 75005 Paris, France
[2]LadHyX, CNRS UMR 7646, École polytechnique, 91128 Palaiseau, France

We study the behaviour of elongated puddles deposited on non-wetting substrates. Such liquid strips retract and adopt circular shapes after a few oscillations. Their thickness and horizontal surface area remain constant during this reorganization, so that the energy of the system is only lowered by minimizing the length of the contour (and the corresponding surface energy); despite the large scale of the experiments (several centimetres), motion is driven by surface tension. We focus on the retraction stage, and show that its velocity results from a balance between the capillary driving force and inertia, due to the frictionless motion on non-wetting substrates. As a consequence, the retraction velocity has a special Taylor–Culick structure, where the puddle width replaces the usual thickness.

Key words: capillary flows, drops and bubbles, interfacial flows (free surface)

1. Introduction

Liquid interfaces carry surface energy, a well-known consequence of the cohesion of fluids. Hence, a liquid volume tends to minimize its surface area, which results in spheres in the absence of gravity: droplets in clouds and bubbles in champagne are all spherical. Plateau (Plateau 1873; Lord Rayleigh 1892; Eggers 1997) showed that stretching this shape generates a force bringing the system back to its optimum state, as we can see when elongating a spring (von Segner 1751; Maxwell 1898). Indeed, the surface tension γ of a liquid can be viewed as the stiffness of a spring (with which it shares dimensions, namely N m^{-1}), and the corresponding force is expressed by multiplying γ by an appropriate length scale. We propose here to conduct Plateau-type experiments with liquids lying on solids, and consider for this purpose non-wetting materials for which the solid/liquid contact is minimized, so that phenomena can be studied without pinning (which could maintain metastable deformations) and with limited friction (approaching the frictionless motion of liquids surrounded by air only).

† Email address for correspondence: david.quere@espci.fr

We consider puddles, that is, large amounts of liquid flattened by gravity, for which we do not expect surface tension to play the role it has at smaller scales. We investigate what happens when a puddle is stretched so as to form a liquid strip, and whether/how it retracts as a Plateau drop and a rubber band do if elongated (Vermorel, Vandenberghe & Villermaux 2007). We discuss the force driving it to a less energetic state, and the dynamics of the process. These experiments can be compared with the retraction after bursting of thin liquid sheets, either inviscid (Taylor 1959; Culick 1960) or viscous (Debrégeas, Martin & Brochard-Wyart 1995; Debrégeas, de Gennes & Brochard-Wyart 1998), studies recently developed by Brenner & Gueyffier (1999), Sünderhauf, Raszillier & Durst (2002) and Savva & Bush (2009). However, thin films retract because of a direct action of surface tension that tends to make these films eventually thicker and more globular (Taylor 1959; Culick 1960; Debrégeas *et al.* 1995), while puddles, when retracting, should keep a constant thickness due to gravity, which impacts both the driving force and the associated dynamics.

2. Observations

Water is deposited on superhydrophobic materials consisting of polished brass coated by a thin layer of hydrophobic colloids (Glaco Mirror Coat Zero). Distilled water meets these substrates with an advancing angle of $\theta_A \approx 171 \pm 2°$ and a receding angle of $\theta_R \approx 165 \pm 2°$. These high values and the corresponding low hysteresis $\Delta\theta = \theta_A - \theta_R \approx 6°$ characterize a superhydrophobic Cassie state: liquid only contacts the tops of the hydrophobic colloids, which minimizes the pinning of contact lines and viscous dissipation (Gogte *et al.* 2005; Olin *et al.* 2013; Dupeux *et al.* 2014). In such a state, the height H of a puddle becomes nearly independent of the contact angle and it tends towards twice the capillary length $2a = 2(\gamma/\rho g)^{1/2}$ (i.e. approximately 5 mm for water), where ρ is the liquid density and g is the acceleration of gravity (de Gennes, Brochard-Wyart & Quéré 2004).

After depositing 1–10 ml of water (or water/glycerol mixture) on the substrate, the resulting circular puddle is elongated using two copper bars of rectangular cross-section. These bars, which are cleaned with acetone and ethanol, are decorated with silver bumps by an immersion of 20 s in a 0.01 M solution of $AgNO_3$, following the procedure by Larmour, Bell & Saunders (2007). The resulting rough surface is highly hydrophilic, allowing the bars to stick to water and to elongate the puddles. We keep the holders at a given distance, and use a micropump and a needle to decrease/increase the volume of liquid, until the main contact lines become aligned along the axial direction of the elongated puddle. By changing the size and distance of the two holders, we obtain strips of initial width W_0 and length L_0, as defined and shown in figure 1. At large W_0, the water is very sensitive to gravity, so that tiny perturbations make it slide away from the substrate, whose horizontality is adjusted with micrometric screws below the flat substrate. Conversely, thin cylinders of small W_0 cannot be captured, because the high value of the Laplace pressure allows them to escape from the holders. In summary, W_0 is varied between 7.5 and 30 mm, with a corresponding aspect ratio $r = L_0/W_0$ typically between 5 and 10.

After elongating a puddle, the holders are rapidly removed and the free strip is observed either from the top or from the side using a high-speed video camera (Phantom V7) at 1000 f.p.s. The experiments are all carried out at room temperature. We show in figure 1 the evolution of a strip of volume $\Omega = 5.7$ ml and initial aspect ratio $r = L_0/W_0 \approx 5$. Once the holders are removed (which defines $t = 0$), both ends retract and the liquid adopts a dumbbell shape ($t \approx 0.11$ s). The converging flow
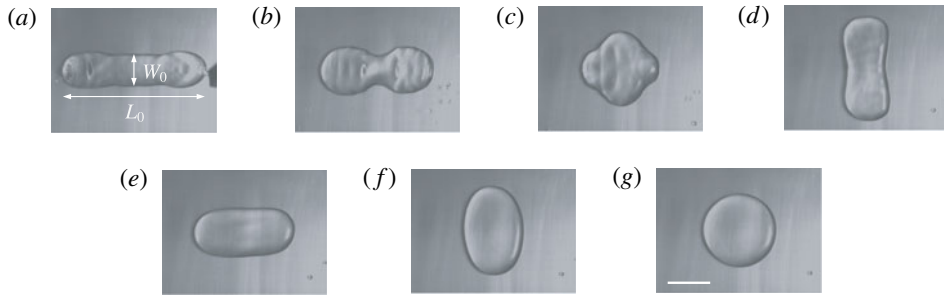
FIGURE 1. Top view of the relaxation of an elongated puddle of water of volume $\Omega = 5.7$ ml deposited on a superhydrophobic material. The initial width and length of the liquid strip are $W_0 = 15$ mm and $L_0 = 70$ mm respectively. We focus in this paper on the initial retraction stage ($t < 0.2$ s): (a) $t = 0$, (b) 0.11 s, (c) 0.24 s, (d) 0.39 s, (e) 0.87 s, (f) 1.34 s, (g) 1.94 s. The scale bar shows 20 mm.

produces a rebound along the perpendicular axis (0.24–0.39 s), and oscillations are observed (with a typical period $\tau \approx 0.4$ s) until equilibrium is reached ($t \approx 2$ s). The final puddle of perimeter C_f is circular, which suggests that surface tension drives the collapse. The oscillations also suggest that the dynamics results from a balance between surface tension and inertia. Denoting L as a characteristic distance, this balance can be written as $\rho \Omega L / \tau^2 \sim \gamma L$, from which we obtain $\tau \sim (\rho \Omega / \gamma)^{1/2}$, i.e. 0.3 s for the parameters used in figure 1, indeed close to the period observed for the oscillations.

3. Retraction of the strip

We focus in this paper on the first stage of evolution (typically between $t = 0$ and $t = 0.2$ s in figure 1), prior to the first oscillation. In this stage, the strip collapses with a well-defined shape, as seen in figure 2(a), where we report top and side views of the retraction and the corresponding contours for $L_0/W_0 \approx 5.6$ and $W_0/a = 7.7$. As the strip shrinks, two rounded regions appear at the ends and grow, while W_0 remains constant in the central part. Waves at the surface superimpose on the global motion, and the sequence lasts until the circular regions merge. The retraction is symmetric, and we denote U as its typical velocity, as defined in figure 2(a). Side views at the same stage for similar parameters ($L_0/W_0 \approx 5.6$ and $W_0/a = 7.8$) show that the mean thickness remains constant during retraction, keeping the value $H \approx 2a$ of static puddles on non-wetting substrates. We can extract from the contours different characteristic distances such as the length L of the central part or the typical radius R of the rounded regions. We deduce from the experiments in figure 2(a) the temporal variations of the length L of the central part, of the total length $L + 4R$ and of the average characteristic length $L + 2R$. As seen in figure 2(b), these distances vary roughly as linear functions of time. A typical retraction velocity is deduced from the average curve $L(t) + 2R(t)$. We find $2U = 14.1 \pm 0.5$ cm s^{-1}, where the factor 2 comes from the symmetric retraction of the strip, whose ends both shrink at a velocity U, as defined in figure 2(a).

We display in figure 2(c) how the geometrical characteristics of the retracting strip vary as X increases. Once extracted from the contours and side views, both the surface area A and the height h_c of the gravity centre of the puddle are observed to change by less than 5 % during the retraction stage. The liquid strip keeps a constant thickness
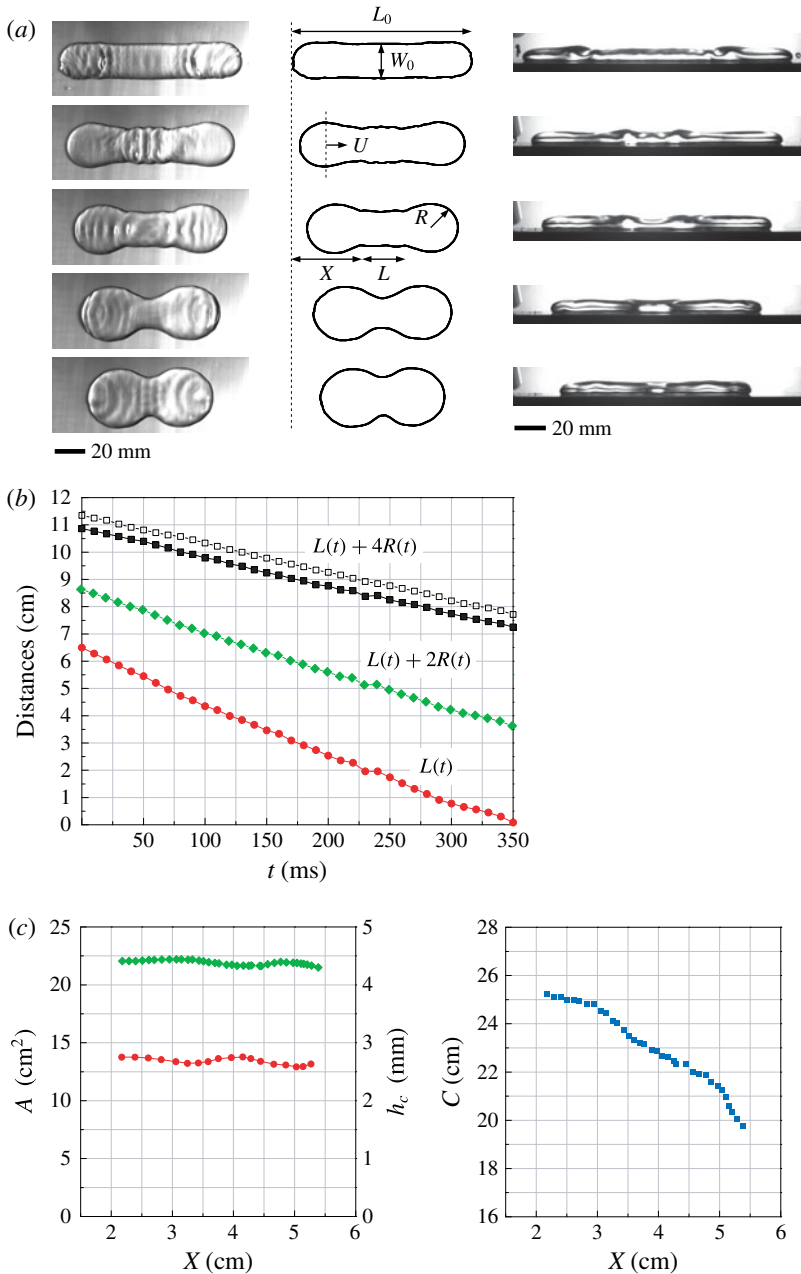
778 R6-3

FIGURE 2. (*a*) Retraction of a water strip seen from the top and from the side. The puddles have an initial width of $W_0 = 21$ mm and an initial length of $L_0 = 110$ mm or 114 mm. The time interval between snapshots is 0.08 s. (*b*) We extract from the contours the total length of the puddle $L + 4R$ (squares), the distance between end centres $L + 2R$ (diamonds) and the length L of the central part (circles), all plotted as a function of time. The solid and hollow symbols correspond to top and side views. (*c*) Variations of the geometrical characteristics of the strip as it retracts. The surface area A of the liquid (seen from the top) and the height h_c of the centre of gravity (deduced from side views) both vary by less than 5 %. In contrast, the perimeter C of the puddle (measured from top views) decreases by 22 % during retraction.
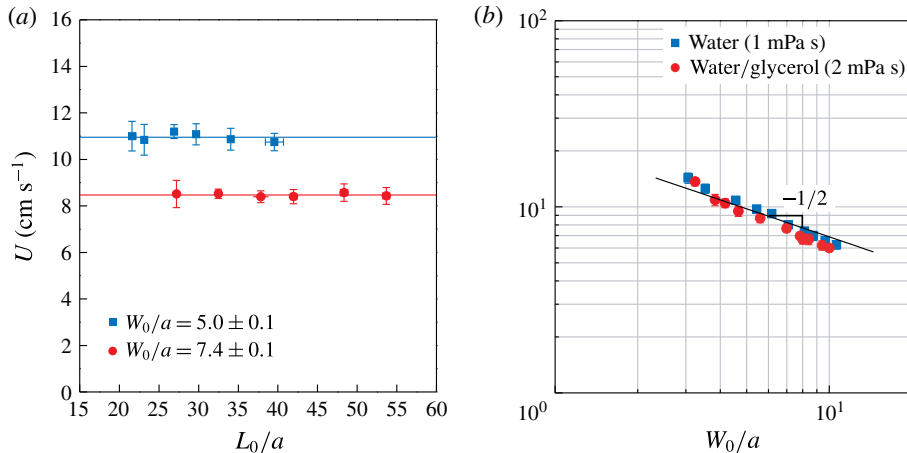
FIGURE 3. (*a*) Typical retraction velocity U as a function of the initial length L_0 of the strip for two widths W_0. (*b*) Velocity U as a function of the strip width W_0 for water (blue data) and for a mixture of water and glycerol two times more viscous (red data).

$H \approx 2a$, as already noted in figure 2(*a*). Hence, its projected surface area A (the one visible in the top views) must indeed remain constant, a consequence of volume conservation $\Omega \approx AH \approx 2Aa$. We deduce that both the potential energy and the surface energy associated with the top and bottom interfaces hardly change during retraction. In sharp contrast to these facts, the puddle perimeter C strongly decreases during the retraction stage. We observe in figure 2(*c*) a decrease from its initial value C_0 by approximately 22 %, a significant amount of the total reduction of the perimeter $(C_f - C_0)/C_0$, of the order of 35 % in figure 1. The ratio C_f/C_0 between the final and initial perimeters is expected to be $(\pi r)^{1/2}/(r+1)$, that is, a quantity of 66 % for an aspect ratio of $r = 5$. For 10 experiments with r between 4.5 and 6, we measure an average ratio C_f/C_0 of 68 %, in excellent agreement with the expectations. We also checked for the same experiments that the final surface area of the puddle remains that of the initial strip (variation less than 5 %).

We measured the mean speed of retraction of strips of various initial lengths L_0 and widths W_0, using as the liquid water and a mixture of water and glycerol two times more viscous. For each strip, we determined the characteristic retraction speed U defined in figure 2(*a*), that is, half the slope of the curve $L(t) + 2R(t)$ in figure 2(*b*). The results are displayed in figure 3, where each data point corresponds to an average of five measurements. Figure 3(*a*) shows that the speed U is independent of the initial length L_0 of the liquid strip (varied by a factor of 3). Data plotted for two initial widths W_0 suggest that wider strips retract more slowly.

The speed U is plotted for two liquid viscosities (that of water, and two times larger) in figure 3(*b*), as a function of the puddle width W_0. Decreasing the width by a factor of approximately 4 leads to an increase of the retraction speed by a factor of the order of 2. The dynamics is found to be the same for both liquids, which confirms an inertial origin for the resistance to motion. When using a mixture of water and glycerol 10 times more viscous than water, the speed U is approximately 25 % smaller, showing the appearance of (weak) viscous corrections at such viscosities.
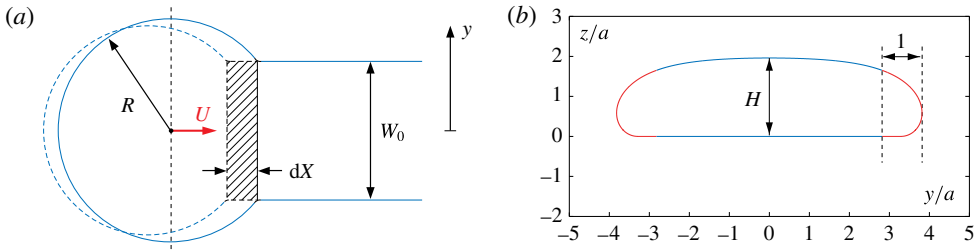
FIGURE 4. (*a*) The end of a retracting strip is sketched as a circular disk of radius R whose centre moves at velocity U, and connected to a static part of width W_0. The sketch represents the puddle at two successive moments, corresponding to a retraction by a distance dX of half the strip. (*b*) Numerical cross-section of a non-wetting strip of width $W_0 = 8a$, where we stress in red the curved boundary close to the edges. Here, z is the vertical coordinate and a is the capillary length.

4. Model and discussion

The cause of retraction appears to be different from what happens for the usual retraction (or bursting) of thin liquid films, for which the planar surface area decreases and the thickness eventually increases. Here, these quantities are constant, and only the perimeter is found to decrease along the motion (figure 2*c*), suggesting that the retraction is driven by the strip sides. Our system is sketched in figure 4(*a*), where each part of the retracting strip seen from the top is assumed to be the juxtaposition of a disk of radius R with a central ribbon of constant width W_0 and (decreasing) length L. As soon as retraction starts, we have $2R > W_0$, as observed in figure 2(*a*). We also display in figure 4(*b*) a numerical cross-section of a non-wetting strip of width $W_0 = 8a$ (chosen to correspond to figure 2*a*), whose thickness H is found to be very close to its asymptotic value $2a$.

Since the puddle thickness is proportional to the capillary length a, its perimeter C holds a surface energy E scaling as $\gamma a C$, which is minimum when $C(X)$ is minimum, that is, for a circular shape. The force F deriving from this energy drives retraction and it scales as γa. Although the puddle shape is dictated by gravity, retraction is driven by surface tension and F appears to be a strong function of γ (varying as $\gamma^{3/2}$), since a higher γ generates a thicker film, whose edges hold more surface energy.

As observed in figure 3(*b*), the origin of the force opposing capillary action is not viscous: we deal with non-wetting substrates, hence minimizing the contributions of line friction (viscous force associated with the motion of contact lines) and bulk friction (the puddles are millimetre thick and made of water). The typical velocities are approximately 10 cm s^{-1} and the strips are centimetric, which yields Reynolds numbers during retraction of the order of 10^3 for water; inertia is the main source of resistance to motion. The mass flux dM/dt of water feeding each end scales as $\rho a W_0 U$, so that Newton's law d(MU)/d$t = F$ has a very simple solution of constant velocity, scaling as

$$U \sim \left(\frac{\gamma}{\rho W_0} \right)^{1/2}. \tag{4.1}$$

Equation (4.1) captures most observations. Retraction indeed takes place at a roughly constant velocity (figure 2*a,b*). This velocity is independent of the strip length L_0, and it decreases with its width W_0 (figure 3). The straight line of slope $-1/2$ in

778 R6-6

the logarithmic plot of figure 3(*b*) agrees fairly well with the data. In addition, the value of the velocity predicted by (4.1) for water and centimetric width is of the order of 10 cm s^{-1}, as observed experimentally. More generally, (4.1) is a kind of Taylor–Culick equation (Taylor 1959; Culick 1960): a (soap) film of thickness h also retracts at constant velocity, a consequence of similar balance between inertia and surface tension. However, a Culick–Taylor velocity scales as $(\gamma/\rho h)^{1/2}$, a quantity sensitive to the film thickness, which is not found in (4.1). As the strip retraction is driven by a minimization of their perimeter, the film thickness enters in both resisting and driving forces, which explains how the retraction speed can be independent of the thickness a. Yet a distance is needed to construct an inertia–capillary speed, and this distance is found in (4.1) to be the strip width W_0, a large quantity compared with the thickness, which explains why the strip retraction is significantly slower than that of films.

Beyond scaling laws, it is not easy to build a fully quantitative model, mainly because an analytical solution only exists in the asymptotic regime of very long strips – an experiment difficult to perform. In such an ideal case, the retracting ends swallow four lateral edges, so that we expect $dC/dX \approx -4$. A first approximation for the edge cross-section consists of describing it by a hemicircular meniscus of radius a, which implies that each edge carries an energy per unit length of $\pi\gamma a$. This can be refined, and we can numerically calculate the extra-surface area corresponding to each edge by imposing a cutoff distance a from the edge (red part in figure 4*b*). Then we find $2.9\gamma a$, close to the previous value, which we adopt. Deriving the corresponding surface energy of edges $E(X) \approx \gamma\pi a C(X)$, we find a force $F = -(1/2)\,dE/dX$ acting on each edge $F \approx 2\pi\gamma a$. Introducing the (varying) mass M of a circular end, Newton's law can be written as

$$\frac{\mathrm{d}}{\mathrm{d}t}(MU) = 2\pi\gamma a. \tag{4.2}$$

We have $dM/dt = 2\rho a W_0 U$, so that (4.2) has a solution of constant velocity:

$$U = \left(\frac{\pi\gamma}{\rho W_0}\right)^{1/2}, \tag{4.3}$$

which obeys the scaling of (4.1).

In our experiments, we are not yet in this asymptotic regime, which complicates a quantitative analysis, the main question being to determine how the strip perimeter decreases as it retracts. However, we have an experimental answer to this question, as seen in figure 2(*c*): the variation of $C(X)$ starts with a short plateau and then gradually bends down, without reaching the slope -4 discussed above. Considering an average slope across the data in figure 2(*c*) of -1.5, the effective force driving the motion in this regime is approximately two times smaller than discussed above. The origin of this reduction can be understood. As half of the puddle retracts by a distance dX at constant thickness $H = 2a$, as sketched in figure 4(*a*), conservation of volume imposes (for R larger than W_0)

$$W_0\,\mathrm{d}X \approx 2\pi R\,\mathrm{d}R. \tag{4.4}$$

During this motion, the perimeter of the puddle decreases by a quantity dC:

$$\mathrm{d}C \approx -4\,\mathrm{d}X + 4\pi\left(\frac{\partial R}{\partial X}\right)\mathrm{d}X \approx -4(1 - W_0/2R)\,\mathrm{d}X. \tag{4.5}$$

778 R6-7

The function $1 - W_0/2R(X)$ varies slowly and its mean value in our experiment is 0.35, significantly smaller than 1, which implies from (4.5) a decrease of perimeter dC/dX of approximately -1.4, close to the measured value. Hence, the effective force driving the motion of one end, $F \approx -\gamma \pi a < dC(X)/dX > /2$, is smaller than $2\gamma \pi a$, its value at large time. Balancing this mean force with inertia yields a velocity scaling as in (4.1), with a numerical coefficient of 1.1, slightly smaller than expected from (4.3), and in fair agreement with the numerical coefficient in the fit of figure 3(*b*), which is 1.3.

These considerations also help us to understand why the velocity V at which the whole puddle retracts (the slope of the square data in figure 2*b*) differs from U. As motion takes place, the circular ends grow at a rate $\dot{R} = dR/dt$, which imposes $V = U - \dot{R}$. The rate $\dot{R}$ can be deduced from (4.4), which yields $\dot{R} = W_0 U/2\pi R$, that is, U/π close to the beginning of the motion ($R \approx W_0/2$). In this limit, U and V are quite different, since we have $V \approx U(1 - 1/\pi) \approx 0.7U$, in fair agreement with the ratio ~ 0.75 observed between the slopes in figure 2(*b*). For a strip of very large aspect ratio, we expect both velocities to become similar, a regime not reached in our experiments where L_0/W_0 remains smaller than 10.

5. Conclusion

A water strip on a slippery horizontal substrate was found to retract under the action of the surface energy associated with its edges. The mechanism of retraction is different from the usual ones reported in the context of thin films, where dewetting or bursting leads to a thickening of the film. We could see our experiment viewed from the top as a (huge) magnification of thin-film retraction seen from the side, where the strip width plays the role of the film thickness. In both cases, a rim forms and progresses, and its inertia limits its speed so that a Culick expression is found. For thin films, however, the contribution of the surface energy of the rim is neglected, while it was found here to lower the force driving retraction. On more common substrates (partial wetting situation), the puddles will be thinner, and the friction opposing the action of surface tension (if the puddles are distorted) should have a viscous origin, either within the bulk of the liquid or close to the contact lines, depending on the puddle size and the contact angle. Hence, we would obtain different dynamics in this case, or even no dynamics at all if pinning becomes dominant, allowing the puddle to remain in metastable distorted states. Extension of our results to such situations of partial wetting remains to be studied.

Acknowledgements

References

BRENNER, M. P. & GUEYFFIER, D. 1999 On the bursting of viscous films. *Phys. Fluids* **11**, 737–739.

CULICK, F. E. C. 1960 Comments on a ruptured soap film. *J. Appl. Phys.* **31**, 1128–1129.

DEBRÉGEAS, G., DE GENNES, P.-G. & BROCHARD-WYART, F. 1998 The life and death of "bare" viscous bubbles. *Science* **279**, 1704–1707.

DEBRÉGEAS, G., MARTIN, P. & BROCHARD-WYART, F. 1995 Viscous bursting of suspended films. *Phys. Rev. Lett.* **75**, 3886–3889.

DUPEUX, G., BOURRIANNE, P., MAGDELAINE, Q., CLANET, C. & QUÉRÉ, D. 2014 Propulsion on a superhydrophobic ratchet. *Sci. Rep.* **4**, 5280.

EGGERS, J. 1997 Nonlinear dynamics and breakup of free-surface flows. *Rev. Mod. Phys.* **69**, 865–929.

DE GENNES, P.-G., BROCHARD-WYART, F. & QUÉRÉ, D. 2004 *Capillarity and Wetting Phenomena: Drops, Bubbles, Pearls and Waves*. Springer.

GOGTE, S., VOROBIEFF, P., TRUESDELL, R., MAMMOLI, A., VAN SWOL, F., SHAH, P. & BRINKER, C. J. 2005 Effective slip on textured superhydrophobic surfaces. *Phys. Fluids* **17**, 051701.

LARMOUR, I. A., BELL, S. E. J. & SAUNDERS, G. C. 2007 Remarkably simple fabrication of superhydrophobic surfaces using electroless galvanic deposition. *Angew. Chem. Intl Ed. Engl.* **46**, 1710–1712.

LORD RAYLEIGH 1892 On the stability of cylindrical fluid surfaces. *Phil. Mag.* **34**, 177–180.

MAXWELL, J. C. 1898 *Encyclopedia Britannica*, 9th edn. vol. 5, pp. 68–69. Adam and Charles Black.

OLIN, P., LINDSTRÖM, S. B., PETTERSSON, T. & WÅGBERG, L. 2013 Water drop friction on superhydrophobic surfaces. *Langmuir* **29**, 9079–9089.

PLATEAU, J. 1873 *Statique Expérimentale et Théorique des Liquides*. Gauthier-Villars.

SAVVA, N. & BUSH, J. W. M. 2009 Viscous sheet retraction. *J. Fluid Mech.* **626**, 211–240.

VON SEGNER, J. A. 1751 De figuris superficierum fluidarum (nature of liquid surfaces). *Comment. Soc. Reg. Scient. Gottingensis* **1**, 301–372.

SÜNDERHAUF, G., RASZILLIER, H. & DURST, F. 2002 The retraction of the edge of a planar liquid sheet. *Phys. Fluids* **14**, 198–208.

TAYLOR, G. I. 1959 The dynamics of thin sheets of fluid. III. Disintegration of fluid sheets. *Proc. R. Soc. Lond.* A **253**, 313–321.

VERMOREL, R., VANDENBERGHE, N. & VILLERMAUX, E. 2007 Rubber band recoil. *Proc. R. Soc. Lond.* A **463**, 641–658.